Journal of Naval Architecture and Marine Engineering
June, 2021
http://doi.org/10.3329/jname.v18i1.52518 *http://www.banglajol.info*

MATERIAL BEHAVIOUR IN MICROPOLAR FLUID OF BROWNIAN MOTION OVER A STRETCHABLE DISK WITH APPLICATION OF THERMOPHORETIC FORCES AND DIFFUSION-THERMO

Silpi Hazarika[1], Sahin Ahmed[2]
[1]Department of Mathematics, Rajiv Gandhi University, Arunachal Pradesh, India, 791112, Email: silpi.hazarika@rgu.ac.in,
[2]Department of Mathematics, Rajiv Gandhi University, Arunachal Pradesh, India, 791112, Email: sahin.ahmed@rgu.ac.in,

Abstract:

To study the material behavior of axisymmetric flow in micropolar fluid for exchange of heat/mass in a disk placed over permeable regime taking into account the effect of heat generation, diffusion thermo, Brownian motion and thermophoretic effect. A suitable similarity transformation is adapted to convert the governing PDEs to non-dimensional form. A well-tested, numerically stable MATLAB code in connection with Bvp4c is employed for the conservation of equations. The noticeable features of the relevant parameters on micropolar fluid flow for axial velocity, radial velocity, micro-rotation, temperature and species concentrations profiles are accentuated on the plots using MATLAB. It is found that angular velocity is enhanced for augmentation in material parameter. Moreover, due the effect of thermophoretic force, the thickness of thermal and concentration boundary layer are enhanced. In addition, thermal diffusion becomes more for augmented vortex viscosity, and an amplified thermal and molar concentration boundary layer thicknesses can be found. This study incorporates numerous engineering applications on rotating machineries, spin-coating, centrifugal pumps, computer storage devices, chemical engineering and different aerodynamic issues. Also, this analysis signifies great impact on biomechanics and stenosis related issue in medical sciences.

Keywords: Axisymmetric flow, micropolar fluid, material variables, Brownian motion, thermophoretic force, diffusion thermo.

NOMENCLATURE

B_0	magnetic field strength	S_g	spin gradient viscosity parameter
B_{m}	Brownian motion parameter	T	dimensional temperature of the micropolar fluid, K
$\mathbb{C}$	dimensional concentration of the fluid, mol/ m^3	T_0	temperature at the surface of the disk, K
$\mathbb{C}_0$	concentration of the stretching disk, mol/ m^3	T_∞	temperature of the free stream, K
$\mathbb{C}_\infty$	concentration of the free stream, mol/ m^3	T_h	thermophoresis parameter
D_B	mass diffusivity, m^{2}s^{-1}	u, w	dimensional velocity component, m/s
D_H	co-efficient of mass flux, through temperature gradient	V_p	micropolar parameter
D_{f}	Dufour parameter	**Greek Letters**	
$f(\eta)$	non dimensional axial velocity	η	similarity variable
$f'(\eta)$	non dimensional radial velocity	γ	spin gradient viscosity
g^*	acceralation due to gravity, m/s^2	κ	thermal conductivity of fluid, W/(m.K)
$g(\eta)$	non-dimensional angular velocity	μ	viscosity of fluid, kg·m^{-1}·s^{-1}
H_a	magnetic parameter	ν	kinematic viscosity of fluid, kg·m^{-1}·s^{-1}
H_g	heat generation parameter	ω	pseudo-angular velocity, s^{-1}
j	micro inertia density coefficient	ρ	density of the fluid, kg/m^3

1813-8535 (Print), 2070-8998 (Online) Received on: March, 2021

k^*	dimensional vortex viscosity coefficient, Pa.s	(ρC_p)	heat capacitance of the base fluid, J/K
M_p	micro inertia density parameter	$\phi(\eta)$	non-dimensional concentration
M	dimensional angular velocity, s^{-1}	σ	electric conductivity, Sm^{-1}
P_p	porosity parameter	$\theta(\eta)$	non-dimensional temperature
Pr	Prandtl number	(r, ψ, z)	cylindrical polar coordinates
r	radius of the disk, m		
K_p	dimensional porosity		

1. Introduction

Micropolar fluid flow became a popular phenomenon among the researchers for its significant applications and uses in various fields, such as the manufacturing of polymer liquid crystals, drilling of oil, manufacturing of exotic greases, colloidal interruptions, exquisite stones hardening, polymer expulsion, geothermal reservoirs and many more. Eringen (1966, 1972) introduced a theory on micropolar fluids that indicate specific microscopic effects developed by viscous fluids consist of rigid random oriented (or spherical) particles with the support of pressure, body moments and spin inertia. The importance of micropolar fluid is also visualize in the study chemical engineering, environmental sciences, biomedical sciences and geophysical fields.The theory and applications of micro-polar fluids and its importance is presented by Qukaszewicz (1999). Numerous numerical technique for micropolar fluid is developed and discussed by Beg *et al*. (2011). By adding some new concepts to these earlier works, many researchers tried to improve the solutions for micro-polar mixed convective flow through porous over inclined surface with different physical situation Das (2012); Kasim *et al.* (2013) using numerous methodologies.

Micropolar fluid flow and exchange of heat and mass between rotating disks has many practical engineering uses and also a topic interest for the research community. Doh and Muthtamilselvan (2017) examined the effect of flow of micropolar fluid with thermophoretic effect for heat and mass exchange over a rotating disk with uniform magnetic field. The effect of various parameter related to micropolar fluid are discussed by Rauf *et al.* (2015) for axial and radial velocity. We have found many literature on MHD micropolar fluid over rotating disk by Ersoy (1999), Khan *et al*. (2014), Rehman *et al*. (2017), Muhammad *et al*. (2017), Mustafa (2017) and seen their significant technological applications. Takhar et al. (1999, 2000, 2003), Chamkha (1997a, 1997b), Chamkha and Khaled (2000), Chamkha (2000) and Modather et al. (2009) discussed about combined effect of exchange of heat and mass with thermal radiation in various conduits. Ahmed (2010) analytically studied the effect of induced magnetic field for radiating fluid.

It is observed that, due to simultaneous transfer of heat and mass, the Dufour effect is generated. The movements of mass gradient is to create the heat flux, which changes the temperature of the micropolar fluid. Moreover, the mass flux generated due to temperature gradients is the thermal diffusion, which plays an important role in fluid flow. Numerous numerical technique is utilized by the researchers to solve the developed model by them and to get the desired output. Ahmed *et al*. (2014), Zueco *et al*. (2017) developed a 2-D model for exchange of heat and mass and investigated the effects of thermal diffusion and Soret number for a MHD flow.

The motion of random particles, ie. the Brownian motion, which is formed due to the continuous collision of the molecules in the adjoining medium signifies a dynamic role in the area of science and biology. The Brownian motion effect with thermophoresis and viscous dissipation for various nanoparticles is discussed by Hazarika *et al*. (2021), Hazarika and Ahmed (2021), Hazarika *et al.* (2021) and also they put out their conclusions about the effects of nanoparticles volume fractions. Simply, the migration of a huge number of molecules to a macroscopic temperature gradient is known as Thermophoresis and it has a great impact on the study of nanofluid flow. (Sheikholeslami *et al*., 2015) predicted the importances of such effects on nanofluids and conclude that nanofluid temperature is raised with the growth values of Thermophoresis parameter. The model developed by Beg *et al.* (2020), Hsiao (2017), Sabir *et al*. (2020), Hayat *et al*. (2017), Feroz *et al*. (2019) integrate the outcomes of Brownian motion, thermophoresis, Prandtl number, Lewis number and these studies have been considered as important research topics for the wide range of scientific and engineering uses such as, processing of lubrication, cooling and polymer, materials damage due to freezing, food processing. MHD flow of nanofluid with micropolar effect for different significant parameters like suction are discussed by Ezzah *et al*. (2014). They detected that the profiles of velocity and angular velocity rise with the growth of material parameter. Reddy *et al.* (2017) deliberated

the outcomes of MHD boundary layer flow of Cu and Ag nanoparticles with base fluid water with volume fraction taken as 1:4 ratio, in a rotating disk over a porous area for various physical effects. They observed that temperature profiles raised with the accumulative values of nanoparticle volume fraction. The model for heat/mass exchange due to convection and effect of micropolar fluid in a constantly stirring isothermal surface submerged in a medium which is thermally and solutally stratified, is numerically studied by Rashad *et al.* (2014). Rashad and Chamkha (2013) investigated the effect of Soret and Dufour on time dependent angular velocity case for heat/mass exchange of mixed convection flow above a vertical revolving cone in a fluid with the impact of Hartmann number and chemical reaction. Reddy and Chamkha (2016) investigated the effect of thermophoresis on heat and mass transfer flow of a micropolar fluid in the presence of Soret and Dufour effects past a vertical porous plate. Effect of variable viscosity and thermal conductivity for MHD fluid in moving isothermal plate is discussed by Ahmed et al. (2020). Recently, Zemedu and Ibrahim (2020) elaborately discussed the micropolar nanofluid flow over a rotating disk in details through explaining all about the involving parameters.

The novelty of the concerned model is to deliberate the outcomes drawn from the present problem solved numerically by employing MATLAB bvp4c solver and plotted graph using MATLAB code. We have studied the gradients of velocity, temperature and species concentration at the disk and displayed via Tables. Material variables have significant outcomes over the stretching disk and can be communicated with material science and engineering due to stress and strain of the studied micropolar fluid. Furthermore, as diffusion thermo is the phenomenon of transfer of chemicals by motions of molecules, so this study is significant in chemical engineering, and it has a great role in temperature as well as concentration profiles. Diffusion thermo is useful in chemical industry for catalyst design, chemical reactor and to modify the properties of various chemicals. Moreover, to regulate the chemical processes like absorption, extraction and distillation thermodynamics is very essential in chemical engineering.

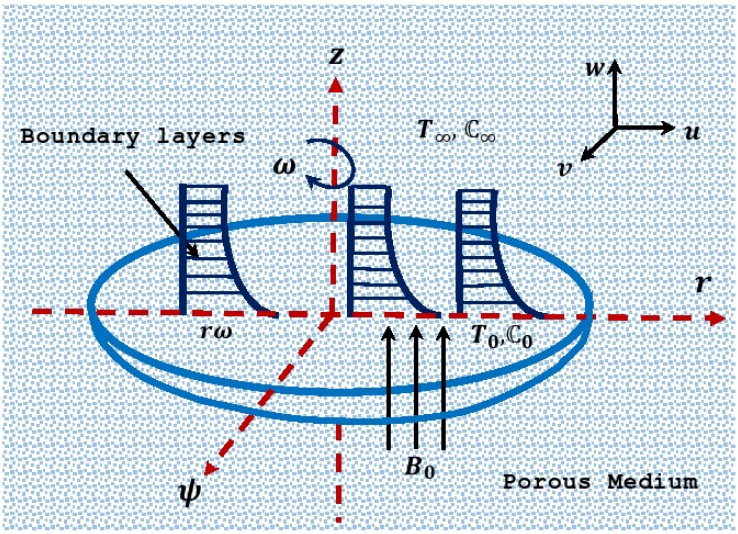

Fig. 1: Flow Model and Coordinate System (Zemedu and Ibrahim, 2020; Rauf *et al*. 2015).

2. Mathematical Formulation

We have considered a steady incompressible electrically conducting micropolar fluid over a disk placed in a porous medium in existence with heat generation, thermophoresis and Brownian motion effects and the flow formation is presented in Fig. 1. We choose a coordinate system in cylindrical co-ordinate as (r, ψ, z), where direction of radius of disk is considered as r-axis and the uniform magnetic field B_0 is placed in the way of z-axis, transverse to the surface of disk. The flow is supposed to be axially symmetric about the vertical z-axis and rotates with angular velocity ω. The velocity and angular velocity components of a fluid particle are respectively considered as (u, v, w) and (N_1, N_2, N_3) in the direction of r, ψ and z. Therefore, due to axially symmetric flow the components of velocity and micro rotation can be chosen as:

$$\begin{Bmatrix} u = u(r,z), v = 0, w = w(r,z) \\ N_1 = 0, N_2 = M(r,z), N_3 = 0 \end{Bmatrix}.$$

The governing equations are (Rauf *et al*. 2015; Zemedu and Ibrahim, 2020):

$$\frac{\partial u}{\partial r}+\frac{\partial w}{\partial z}+\frac{u}{r}=0\,, \tag{1}$$

$$\rho\left(u\frac{\partial u}{\partial r}+w\frac{\partial u}{\partial z}\right)=\left\{\begin{matrix}-\frac{\partial p}{\partial r}-k^{*}\frac{\partial M}{\partial z}+(\mu+k^{*})\left(\frac{\partial^{2}\mathrm{u}}{\partial r^{2}}+\frac{1}{r}\frac{\partial u}{\partial r}-\frac{u}{r^{2}}+\frac{\partial^{2}\mathrm{u}}{\partial z^{2}}\right)\\ -\sigma_{e}{B_{0}}^{2}u-\frac{\mu k_{1}}{K_{p}}u\end{matrix}\right\}, \tag{2}$$

$$\rho j\left(u\frac{\partial M}{\partial r}+w\frac{\partial M}{\partial z}\right)=k^{*}\left(\frac{\partial u}{\partial z}-\frac{\partial w}{\partial r}\right)-2k^{*}M+\gamma\left(\frac{\partial^{2}\mathrm{M}}{\partial r^{2}}+\frac{1}{r}\frac{\partial M}{\partial r}-\frac{M}{r^{2}}+\frac{\partial^{2}\mathrm{M}}{\partial z^{2}}\right), \tag{3}$$

$$\rho C_{p}\left(u\frac{\partial T}{\partial r}+w\frac{\partial T}{\partial z}\right)=\left\{\begin{matrix}\kappa\left(\frac{\partial^{2}\mathrm{T}}{\partial r^{2}}+\frac{1}{r}\frac{\partial T}{\partial r}+\frac{\partial^{2}\mathrm{T}}{\partial z^{2}}\right)-Q_{0}(T-T_{\infty})\\ +\frac{D_{B}K_{T}}{C_{s}}\left(\frac{\partial^{2}\mathbb{C}}{\partial r^{2}}+\frac{1}{r}\frac{\partial\mathbb{C}}{\partial r}+\frac{\partial^{2}\mathbb{C}}{\partial z^{2}}\right)\end{matrix}\right\}, \tag{4}$$

$$u\frac{\partial\mathbb{C}}{\partial r}+w\frac{\partial\mathbb{C}}{\partial z}=D_{B}\left(\frac{\partial^{2}\mathbb{C}}{\partial r^{2}}+\frac{1}{r}\frac{\partial\mathbb{C}}{\partial r}+\frac{\partial^{2}\mathbb{C}}{\partial z^{2}}\right)+\frac{D_{\mathcal{H}}}{T_{\infty}}\left(\frac{\partial^{2}\mathrm{T}}{\partial r^{2}}+\frac{1}{r}\frac{\partial T}{\partial r}+\frac{\partial^{2}\mathrm{T}}{\partial z^{2}}\right)\ , \tag{5}$$

The equations are subjected to the following boundary conditions (Rauf *et al.* 2015):

$$\left.\begin{matrix}u=r\omega,\ \ w=0\,,\ \ M=0\,,\ \ \mathrm{T}=T_{0},\ \ \mathbb{C}=\mathbb{C}_{0}\ \text{ at }\ \ z=0\\ u\to 0\,,\ \ \mathrm{w}\to 0\,,\ \ M\to 0\,,T\to T_{\infty},\mathbb{C}\to\mathbb{C}_{\infty}\text{ as }\ z\to\infty\ ,\end{matrix}\right\}, \tag{6}$$

Variables for similarity transform are stated as

$$\left\{\begin{matrix}\eta=z\sqrt{\frac{\omega}{\nu}}\ , & u=-\frac{r\omega}{2}f'(\eta), & M=\sqrt{\frac{\omega}{\nu}}\,r\omega g(\eta),\\ \mathrm{w}=\sqrt{\nu\omega}f(\eta), & \theta(\eta)=\frac{T-T_{\infty}}{T_{0}-T_{\infty}}\,, & \phi(\eta)=\frac{\mathbb{C}-\mathbb{C}_{\infty}}{\mathbb{C}_{w}-\mathbb{C}_{\infty}}\end{matrix}\right\} \tag{7}$$

Using similarity transformations (7), the converted equations (2) to (5) are

$$\left(1+V_{p}\right)f'''+\frac{f'^{2}}{2}-ff''+2V_{p}g'-(H_{a}+P_{p})f'=0\,, \tag{8}$$

$$M_{p}g''+S_{g}\left(fg'-\frac{f'g}{2}\right)-V_{p}\left(2g+\frac{f''}{2}\right)=0\ , \tag{9}$$

$$\theta''-Prf\theta'-H_{g}\theta+D_{f}\phi''=0\ , \tag{10}$$

$$\phi''-Sc\ f\ \phi'+\frac{T_{h}}{B_{m}}\theta''=0, \tag{11}$$

primes denote differentiation with respect to the similarity variable η .

The concerning non-dimensional parameters are:

$$\left\{\begin{matrix}V_{p}=\frac{k^{*}}{\mu},\ \ M_{p}=\frac{\gamma\omega}{\mu\nu},\ \ S_{g}=\frac{\rho\omega j}{\mu}\,,\ \ {H_{a}}^{2}=\frac{\sigma_{e}{B_{0}}^{2}}{\rho\omega},\ \ P_{p}\ =\frac{\mu k_{1}}{K_{p}\omega},\\ H_{g}=\frac{Q_{0}\mu C_{p}}{\omega\kappa}\,,\ \ B_{m}=\frac{\tau\,D_{B}(\mathbb{C}_{0}-\mathbb{C}_{\infty})}{\nu},\ \ T_{h}=\frac{\tau D_{\mathcal{H}}(T_{0}-T_{\infty})}{T_{\infty}\nu},\\ D_{f}=\frac{D_{B}K_{T}\rho C_{p}(\mathbb{C}_{0}-\mathbb{C}_{\infty})}{C_{s}\kappa(T_{0}-T_{\infty})},\quad Sc=\frac{\nu}{D_{B}}\,,\ \ Pr=\frac{\upsilon C_{p}}{\kappa}\end{matrix}\right\} \tag{12}$$

The reduced boundary conditions are:

$$\left.\begin{matrix}f=0,f'=-2,\ \ g=0\,,\theta=1,\ \ \phi=1\ \text{ at }\ \eta=0\\ f\to 0,f'\to 0\,,g\to 0\,,\theta\to 0,\phi\ \to 0\text{ as }\ \eta\to\infty\ ,\end{matrix}\right\} \tag{13}$$

3. Calculations of Physical Parameters at $\eta = 0$

The coefficient of skin friction, the rate of heat transfer and the rate of mass transfer at the surface in dimensional form are defined as:

$$\overline{C_f} = \frac{2\tau_w}{\rho(r\omega)^2}, \qquad \overline{Nu_x} = \frac{rq_m}{\kappa(T_0 - T_\infty)}, \qquad \overline{Sh_x} = \frac{rJ_w}{D_B(\mathbb{C}_0 - \mathbb{C}_\infty)} \tag{14}$$

where τ_w , q_m and J_w represent the shear stress, heat flux and mass flux at the surface ($z = 0$) respectively, and defined as:

$$\tau_w = \left[(\mu + k^*)\frac{\partial u}{\partial z}\right]_{z=0} + \quad [k^* M]_{z=0} \tag{15}$$

$$q_m = -\kappa \frac{\partial T}{\partial z}\Big|_{z=0} \tag{16}$$

$$J_w = -D_B \frac{\partial \mathbb{C}}{\partial z}\Big|_{z=0} \tag{17}$$

By utilizing the Eqs. (15) – (17), the coefficient of skin friction, the rate of heat transfer and the rate of mass transfer in non-dimensional form are:

$$C_f = -\left(R_{e_x}\right)^{-1}\{1 + V_p\}f''(0),$$
$$Nu_x = -\left(R_{e_x}\right)\theta'(0),$$
$$Sh_x = -\left(R_{e_x}\right)\phi'(0),$$

where R_{e_x} indicates the local Reynold's number $R_{e_x} = r\sqrt{\omega}/\sqrt{\nu}$.

4. Methodology

Here we have adapted bvp4c MATLAB code to resolve Equations (8) – (11) with the help of boundary conditions (13). Generally, a boundary value problem of the form $y' = f(x, y, c)$ subject to the general non-linear, two-point boundary conditions $g(y(a), y(b), c) = 0$ where $a \le x \le b$ is solved by adapting bvp4c. The three stage Lobatto-III [Gonzalez et al. (1995)] a formula is utilized for this finite difference code. The methodology involves two basic functions such as function for first order differential equation and residual function for boundary conditions. For example, we have taken f as $y(1)$, f' as $y(2)$, f'' as $y(3)$, g as $y(4)$, g' as $y(5)$, θ as $y(6)$, θ' as $y(7)$, ϕ as $y(8)$ and ϕ' as $y(9)$. Also for the boundary conditions, we have chosen such as $y0(1) = f(0), y0(2) = f'(2), y1(1) = f(1), y1(2) = f'(1)$ and so on. At the beginning of the program, to solve this problem by bvp4c, we have to put a number of functions like the ODE functions, initial data and parameters value.

5. Validity and Accuracy

For confirmation of the validity of current numerical scheme, we have matched the numerical values with those established by Rauf et al. (2015) on the distribution of θ for V_p at $H_g = 0$ and $H_g = 0.2$ over the surface of the disk and achieved an acceptable agreement. The results obtained are well validated via Table 1.

Table 1: Distribution of θ for V_p and H_g

	Rauf et al. (2015) **at $H_g = 0$ (without heat generation)**		Present model **at $H_g = 0.2$ (with heat generation)**	
	V_p		**V_p**	
η	**1**	**3**	**1**	**3**
0.0	1.00000	1.00000	1.00000	1.00000
1.0	0.63574	0.66117	0.64849	0.67853
2.0	0.38908	0.40469	0.40388	0.42662

3.0	0.19963	0.21820	0.20211	0.23906
4.0	0.01272	0.05361	0.02780	0.08392
5.0	0.00000	0.00000	0.00000	0.00000

6. Results and Discussion

The transformed equations are solved numerically by MATLAB bvp4c with the parameter stated below $Pr = 0.71,\ H_a = 5,\ V_p = 2,\ M_p = 0.5,\ S_g = 0.5,\ B_m = 2,\ T_h = 0.3,\ H_g = 2,\ P_p = 0.2,\ D_f = 0.5, Sc = 0.78$. In addition, we have studied the shear stress, Nusselt number and Sherwood number for different parameter and placed the results in Table 2, 3, and 4 respectively.

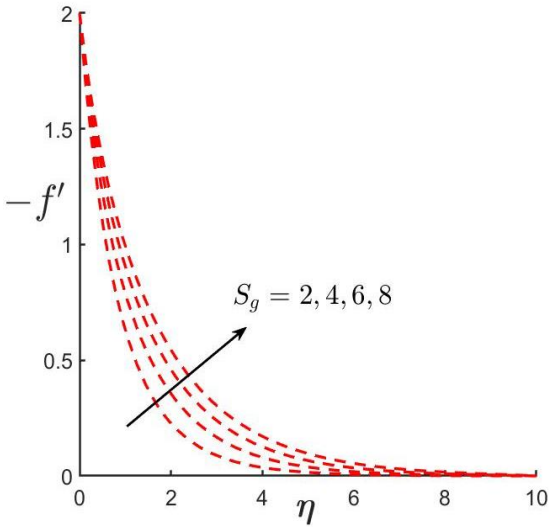

Fig. 2(a): Radial velocity profile for S_g

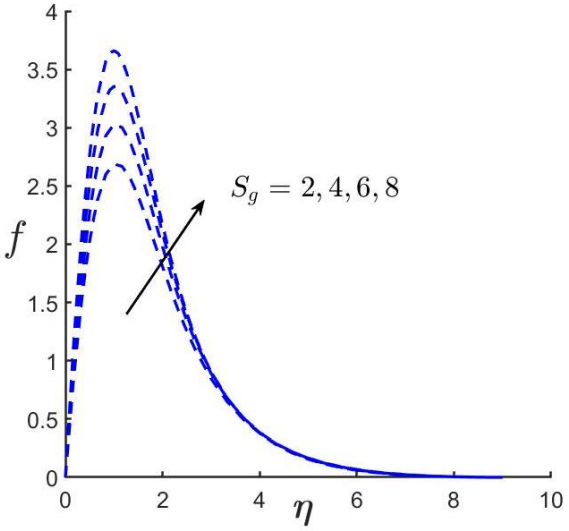

Fig. 2(b): Axial velocity profile for S_g

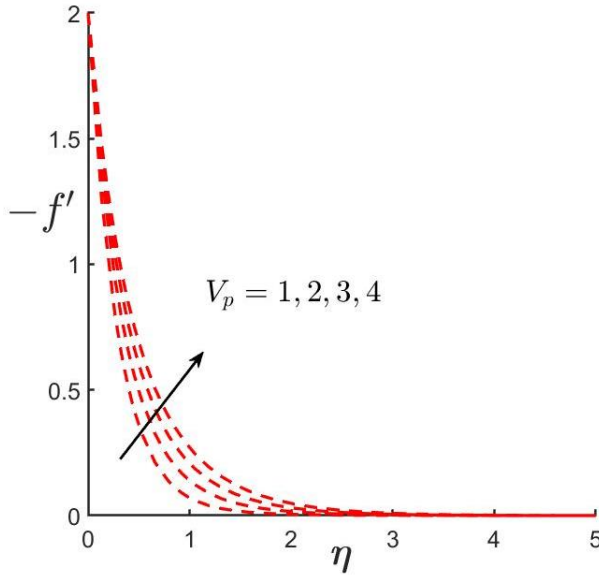

Fig. 3(a): Radial velocity profile for V_p

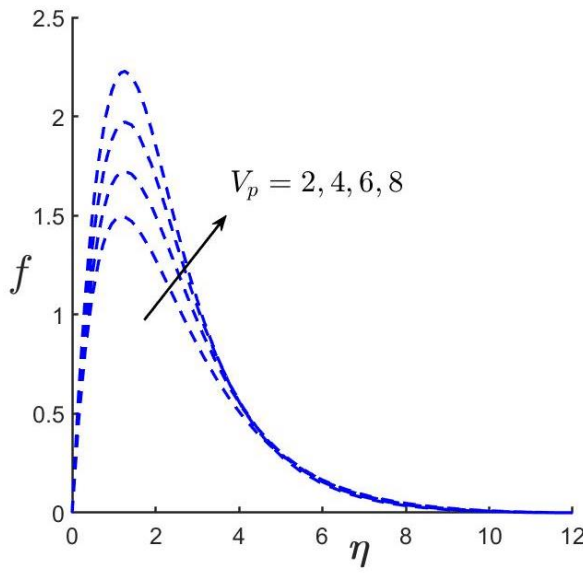

Fig. 3(b): Axial velocity profile for V_p

Figs. 2(a – b) interprets the influence of S_g on the profiles of radial $(-f')$ and axial (f) velocity. It is perceived that the outlines of both the velocities are ran up by rising the values of S_g. Higher spin gradient viscosity boosts the momentum of the molecules of the micropolar fluid in negative direction and hence augmented numerical values are obtained in radial velocity $(-f')$. Maximum enhancing values occurred in $-f'$ towards the direction of

the disk and its corresponding boundary layer width. Similar behaviour has seen in f along the radial direction (transverse to axial).

The impact of V_p on radial $(-f')$ and axial (f) velocity contours are exhibited in Figs. 3(a – b) respectively. It demonstrates that the velocity profiles are amplified by increasing V_p. Applying vortex viscosity (V_p) to the velocity, the heat is generated in the boundary layer and the molecules of fluid transmitted the heat from lower to the higher region and hence the micro-polar parameter accelerated the fluid velocity along axial and radial direction (transverse to axial) and its corresponding boundary layer width. The molecules of the micropolar fluid are travelling along the radial direction when $\eta > 1$.

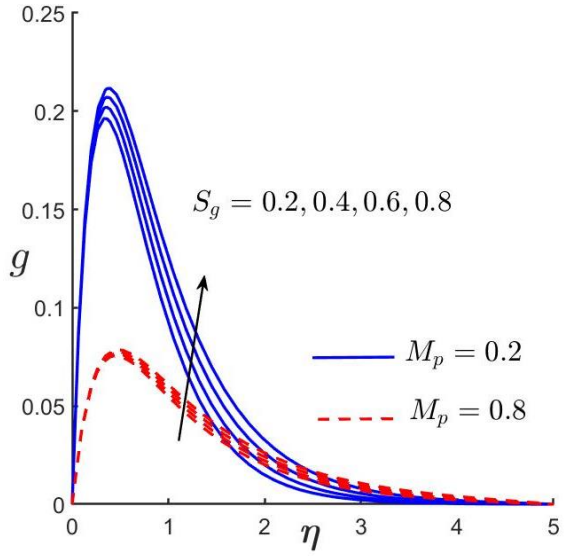

Fig. 4: Angular velocity profile for S_g and M_p

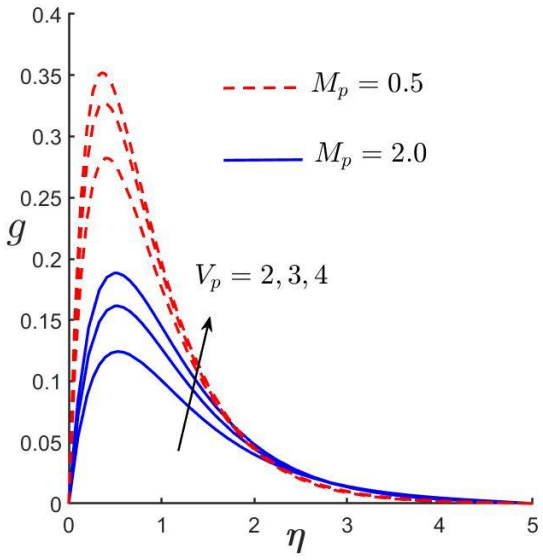

Fig. 5: Angular velocity profile for V_p and M_p

Fig. 4 portrays the effect of S_g and M_p on the contours of angular velocity. It is noted from Fig. 4 that the profiles of g upturn by enhancing the values of S_g, but this effect is reversed for M_p. Also profiles of g boosts near the surface of the disk, and they asymptotically declines far away from the surface. Higher micro-inertia density resists the free movement of molecules of micropolar fluid that leads to the retardation of spin about the vertical axis, while free movement of molecules are available for lower micro-inertia density which accelerates the spin of angular velocity.

The variation of V_p and M_p over the angular velocity is represented by the Fig. 5. The augmented values of the vortex viscosity enhanced the angular velocity very closer to the disk. This elevation of angular velocity has occurred because of weaker stresses of the molecules exerted by the vortex viscosity. Smaller micro-inertia density is dominant over the greater micro-inertia density on the angular velocity as higher V_p physically represents the sluggish motion of the molecules about the axis of rotation.

The impacts of D_f and V_p, on the profiles of θ and ϕ are plotted in the respective Figs. 6(a) and 6(b). Dufour (1873) had deliberated the Dufour effect (D_f) and is the cross-diffusion effect due to simultaneous occurrence of heat and mass transfer in a moving fluid affecting each other. It is represented as $D_f =$ (impact of the concentration gradients) / (thermal energy flux) and it is also termed as diffusion thermo. The trends of concentration gradient is to create the energy flux, which changes the temperature of the micropolar fluid. Here $D_f = 0.1,0.2,0.3,0.4(< 1)$ indicates that thermal energy flux dominant over the concentration gradients and the higher thermal energy boosts the temperature (Fig. 6(a)) of the micropolar fluid for the augmented D_f, while this behaviour on species concentration (Fig. 6(b)) is converse to temperature curves. The D_f can be made significant in binary gas mixtures (Hollinger and Lücke, 1995). Profiles specify that the values of temperature and species concentration enhance with the growth of V_p, because thermal diffusion becomes more due to the rise in the vortex viscosity of the fluid, and an augmented thermal and molar concentration boundary layer thicknesses can be exhibited.

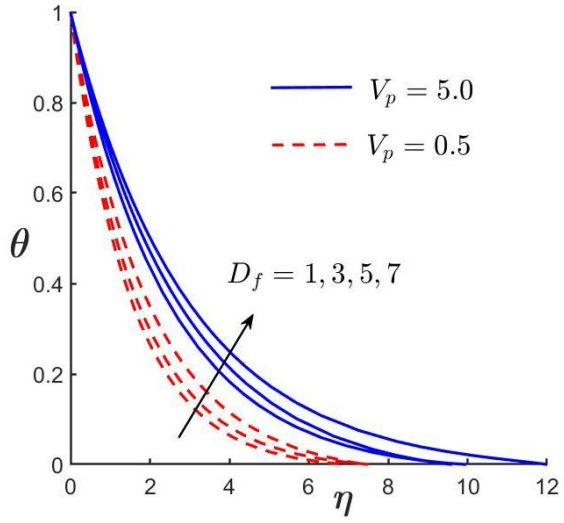

Fig. 6(a): Temperature profile for D_f and V_p

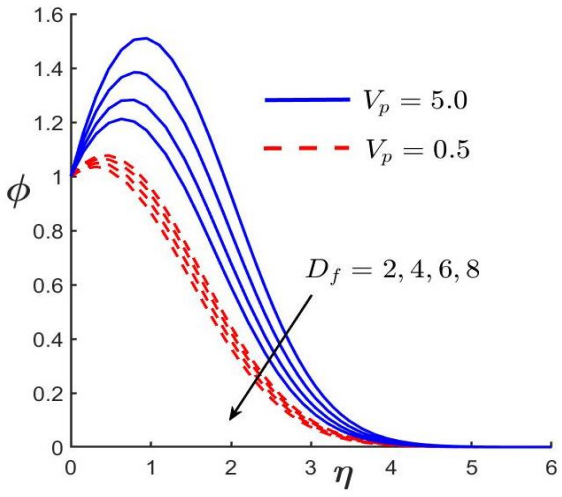

Fig. 6(b): Concentration profile for D_f and V_p

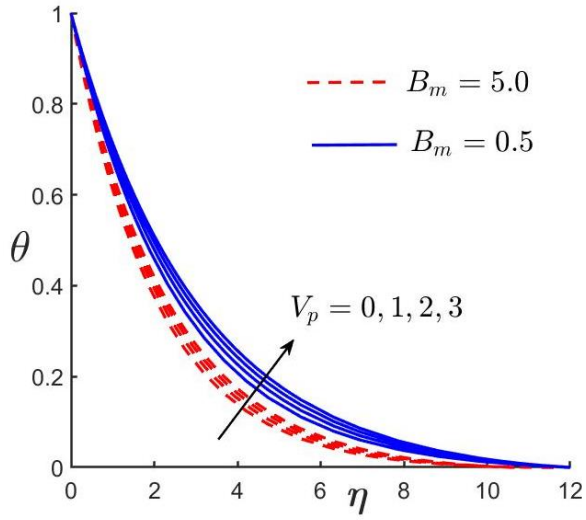

Fig. 7: Temperature profile for V_p and B_m

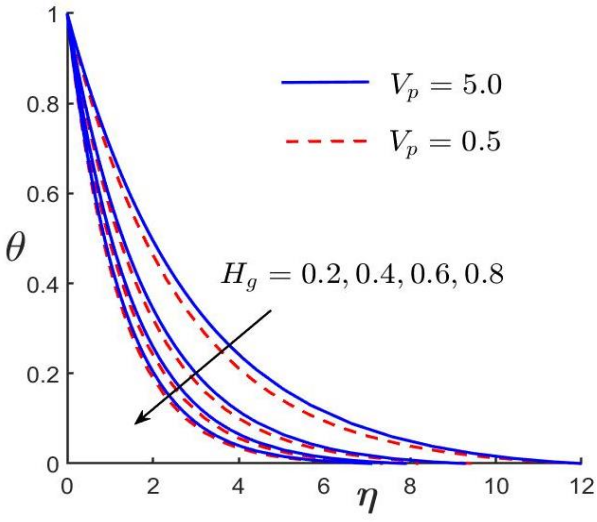

Fig. 8: Temperature profile for H_g and V_p

Fig. **7** indicates the consequence of V_p and B_m on the sketches of g. On improving V_p, the contours of g gets enlarged, but trend is opposite for B_m. Also, when the values of V_p is boosted, the thermal boundary is also enhanced, which heightens the motion of fluid molecules, and results in improving temperature. The thermal motion is a sensation that contains the continuous random bombardment of atoms and molecules in a liquid or gas due to thermal energy, which generates the Brownian motion (Robert Brown, 1828). In lower viscous molecules, smaller size of molecules, and higher temperature, the Brownian motion may develop. The Brownian motion parameter (B_m) is the ratio of the nanoparticle diffusion due to the Brownian motion effect to the thermal diffusion in the nanofluid. According to Einstein-Stokes equation (Buongiorno, 2006), the Brownian motion is proportional to the inverse of the particle diameter and hence the Brownian motion can be enhanced when the diameter of the particle is augmented. Therefore, the augmented B_m declines the fluid temperature. Higher $B_m = 3$ ($\mathbb{C}_0 > \mathbb{C}_\infty$) implicates that the diffusion owing to Brownian motion is dominant over the thermal diffusion and therefore, the thermal boundary layer becomes very thicker than that of lower $B_m = 0.3$ ($\mathbb{C}_0 < \mathbb{C}_\infty$).

The temperature distribution is illustrated in Fig. 8 under the variations of V_p and H_g. In physical point of view, heat always describes the transfer of thermal energy between molecules of the micropolar fluids within a system and it reflects how energy moves or flows. However, fluid temperature describes the average kinetic energy of molecules within a system. It is noted that the amount of heat transferred is directly proportional to the change in

temperature and therefore, the heat is transmitted through higher to lower that the augmented heat generation declining the temperature in micropolar fluid over the disk. In the environment of heat generation, the temperature of the micropolar fluid is escalated for the variation of vortex viscosity. In particular, the thickness of thermal boundary layer becomes very thinner at $V_p = 5.0$ and $H_g = 0.5$.

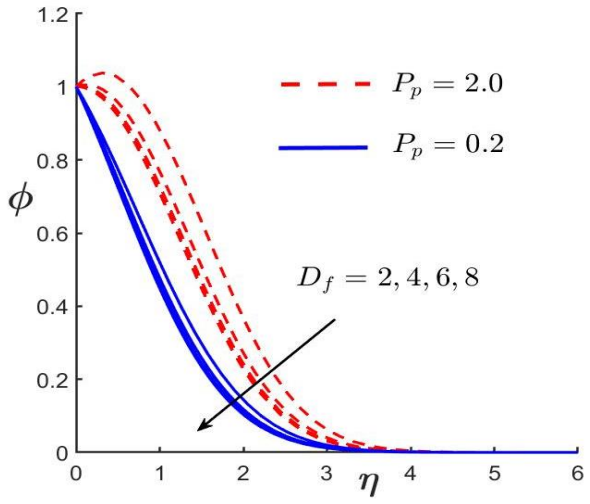

Fig. 9: Concentration profile for D_f and P_p

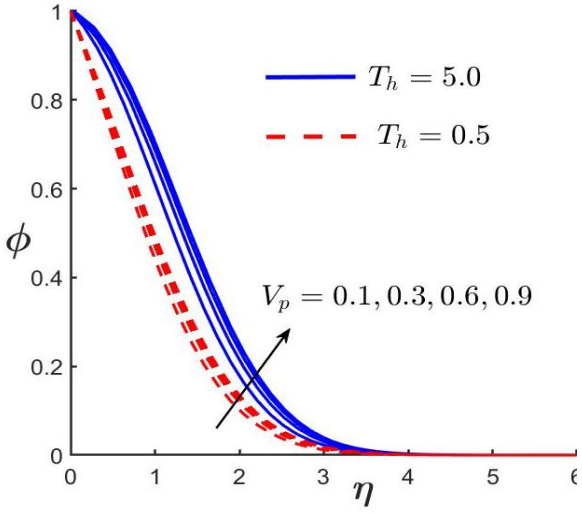

Fig. 10: Concentration profile for V_p and T_h

Fig. 9 shows that the profiles of ϕ for D_f and P_p. In fluid Mechanics, porosity $\boldsymbol{(P_p)}$ of a material is the measurement of its ability to hold a fluid, while permeability is a measurement of the fluid flow easily through a porous material. In practice, a medium may be extremely porous, but the pores are not well connected, then the permeability may not arise in that material. Physically, $\boldsymbol{P_p}$ is the measurement of void spaces in a material and it can be termed as P_p = (volume of pores) / (volume of bulk solid bodies) and is usually expressed as a percentage. Porosity = (Volume of Voids / Total Volume) x 100%. In this investigation, the porosity is based on Darcy's law after the name of Darcy (1856) and is related to the flows of fluid and may be applied in petroleum reservoirs. Also, it may be encountered in geothermal sciences, engineering, biological applications and agriculture. The porosity is always behaves like a drag force which resists the motion of diffusive molecules in the species concentration layers and that implicates the declination in molar concentration (ϕ). It is observed that profiles become decline for larger values of D_f. It is found that a rise in the D_f parameter caused a diminish in the concentration resulting in the movement of molecules from higher concentration to a region of lower concentration which down the concentration gradient. That is why the profiles of ϕ is reduced. In the areas of Hydrology, Petrology and Geosciences, D_f has significant characters.

Fig. 10 displays the effects of V_p and T_h on concentration profiles, respectively. It is seen that contours of ϕ are uplifted significantly for bigger values of V_p and T_h. The phenomenon of Thermophoresis may exit in the combinations of mobile particles, in which the force of a temperature gradient can be observed due to the different responses given by different types of particles. In the physical point of view, thermophoretic forces (T_h) generated the temperature gradient between the heated fluid and the non-heated surface which effects the movement of nanoparticles near the surface. Therefore, T_h is generated the elevated curves and develops the growth of molar species layers. Higher $T_h = 1.0$ ($T_0 > T_\infty$) generates augmented numerical values of ϕ in the molar species layers for the application of vortex viscosity. $T_h = 0.1$ ($T_0 < T_\infty$), which means that the temperature gradient is higher that suppress the motion of molecules and it is opposite to $T_h = 1.0$. diffusion of molar species is least. In absence of vortex viscosity $V_p = 0$, the molar species layers become less thick.

The velocity gradients, temperature gradients and species concentration gradients at the disk ($\eta = 0$) are illustrated in the respective Tables 2, 3, 4 with the impact of material variables and other physical parameters.

Table 2: Distribution of Skin Friction Co-efficient.

Skin Friction (C_f)						
$\boldsymbol{R_{e_x}}$	V_p =1.0	V_p =2.0	$S_g = 0.2$	$S_g = 0.8$	$H_a = 2$	$H_a = 5$
0.1	118.263	177.395	120.622	118.803	45.2854	95.1041
0.2	59.1317	88.6976	60.3114	59.4019	22.6427	47.5520
0.3	39.4211	59.1317	40.2076	39.6013	15.0951	31.7013
0.4	29.5658	44.3488	30.1557	29.7009	11.3213	23.7760

Table 3: Distribution of Rate of Heat Transfer.

Rate of Heat Transfer (Nu_x)						
$\boldsymbol{R_{e_x}}$	T_h =2.0	T_h =4.0	$B_m = 0.4$	$B_m = 0.8$	$H_g = 0.5$	$H_g = 2.0$
0.1	-0.2705	-0.1627	-0.1627	-0.2705	-0.0226	-0.0248
0.2	-0.5410	-0.3255	-0.3255	-0.5410	-0.0453	-0.0496
0.3	-0.8115	-0.4882	-0.4882	-0.81157	-0.0680	-0.0744
0.4	-1.0820	-0.6510	-0.6510	-1.0821	-0.0907	-0.0992

Table 4: Distribution of Rate of Mass Transfer.

Rate of Mass Transfer (Sh_x)						
$\boldsymbol{R_{e_x}}$	T_h =2.0	T_h =4.0	$B_m = 0.3$	$B_m = 0.8$	$V_p = 1.0$	$V_p = 3.0$
0.1	0.72735	0.46256	0.16926	0.46256	0.20348	0.15021
0.2	1.45470	0.92512	0.33857	0.92512	0.40697	0.30042
0.3	2.18206	1.38768	0.50786	1.38768	0.61046	0.45063
0.4	2.90941	1.85024	0.67715	1.85024	0.81395	0.60084

Table 2 describes the distribution of C_f for R_{e_x},V_p, S_g and H_a. C_f is boosted for V_p and H_a. A substantial reduction of C_f is detected for the augmented R_{e_x} and S_g. In Table 3, it is perceived that for the variation of B_m, H_g and R_{e_x}, the rate of heat transfer (Nu_x) is slowed down, while reverse behavioral numerical values of Nu_x arises for T_h. Table 4 signifies that, Sh_x is escalated for higher values of R_{e_x} and B_m, but trend is opposite for V_p and T_h. Materially, Nusselt number is communicated as Nu_x = (Convective Heat Transfer) / (Conductive Heat Transfer). Augmented R_{e_x} falling the curves of Nu_x at $\eta = 0$, which means that the heat is conducted by the molecules from surface to the nanofluid region.

Rayleigh number (R_{e_x}) is calculated as R_{e_x} = (Buoyancy force) / (Thermal diffusivity). Nu_x has exponential decay for augmented R_{e_x} that indicates that heat is exchanged from thermal diffusivity to buoyancy forces in nanofluid region and this behaviour is reversed in Sh_x.

Sherwood number is assigned as Sh_x = (Exchange of mass by convection) / (Exchange of mass by diffusion). An exponential growth is calculated in Sh_x by the swelling R_{e_x}. Adjacent to the disk $Sh_x < 1$ means that diffusion is leading over convection, and away the disk $Sh_x > 1$ that progressively mass is transported through convection to the diffusion.

7. Conclusion

The significant outcomes of the numerically analyzed micropolar hydromagnetic fluid over a disk with thermophoresis and heat generation effect are stated in this section. The conclusions have been picked up for different values of the involving parameters. The prime outcomes of this investigation are as follows:

- The outcomes achieved at this point are beneficial in engineering problems, mostly, in energy systems, rheology, material processing, lubrication and biomedical applications.
- The axial and radial velocity upsurge with the augmented values of V_p and S_g.

- V_p has a weighty impact on temperature as well as on angular velocity.
- There is a rise in magnitude of the profiles of g with an enhancement V_p and S_g near the surface of the disk, but they gradually decay far away from the surface, but g is a decreasing function of M_p.
- The temperature of micro polar fluid has been amplified for the advanced values of V_p and D_f.
- The augmentation of the profiles ϕ is detected for higher values of T_h and V_p, but profiles behave oppositely for D_f and P_p.
- An upsurge in values of R_{e_x} causes reduction in the distribution of C_f and Nu_x, while enhancement is Sh_x.
- At $\eta = 0$, all $Nu_x < 1$ implicates that conduction is dominant over the convection and therefore, heat is transmitted by conduction from surface to the nanofluid region.
- Rayleigh number physically associated with buoyancy-driven flow, so it signifies that the natural convection boundary layer is laminar.
- The persistence of computation of mass flux is to comprehend, and possibly design or control in the system of exchange of mass and it occurs in absorption, evaporation, drying precipitation and distillation.

References

Ahmed, S. (2010): Induced Magnetic field with Radiating Fluid over a Porous vertical plate: Analytical Study, Journal of Naval Architecture and Marine Engineering, Vol. 7, pp. 83-94. http://doi.org/10.3329/jname.v7i2.5662.

Ahmed, S., Abdul, B., Chamkha, A.J. (2014): Finite difference approach in porous media transport modeling for magnetohydrodynamic unsteady flow over a vertical plate Darcian model, International Journal of Numerical Methods for Heat and Fluid Flow, Vol. 24 No. 5, pp. 1204-1223, https://doi.org/10.1108/HFF-01-2013-0008.

Ahmed, S, Hazarika, G. C., Gogoi, G. (2020): Investigation of variable Viscosity and Thermal Conductivity on MHD Mass Transfer flow problem over a moving Non-Isothermal vertical plate, Journal Of Naval Architecture And Marine Engineering, Vol. 17, pp. 183-197. http://doi.org/10.3329/jname.v17i2.48477.

Beg, O.A., Bhargava, R., and Rashidi, M.M. (2011): Numerical Simulation in Micropolar Fluid Dynamics, Lambert Academic Publishing, Germany.

Beg, O. A., Ferdows, M., Karim, M. E., Hasan, M. M., Beg, T. A., Shamshuddin, M., Kadir, A. (2020): Computation of non-isothermal thermo-convective micropolar fluid dynamics in a Hall MHD generator system with non-linear distending wall, International Journal of Applied and Computational Mathematics, Vol. 6, pp. 1–44. https://doi.org/10.1007/s40819-020-0792-y.

Brown, R. (1828): A brief account of microscopical observations made in the months of June, July and August, 1827, on the particles contained in the pollen of plants; and on the general existence of active molecules in organic and inorganic bodies, Philosophical Magazine, Vol. 4, No. 21, pp. 161–173. https://doi.org/10.1080/14786442808674769.

Buongiorno, J. (2006): Convective Transport in Nanofluids, Journal of Heat Transfer, Vol. 128, No. 3, pp. 240-250. https://doi.org/10.1115/1.2150834.

Chamkha, A.J. (1997a): Solar radiation assisted natural convection in uniform porous medium supported by a vertical flat plate, J. Heat Transfer, Vol. 119, No. 1, pp. 89-96. https://doi.org/10.1115/1.2824104

Chamkha, A.J. **(**2000**):** Thermal radiation and buoyancy effects on hydromagnetic flow over an accelerating permeable surface with heat source or sink, International Journal of Engineering Science**,** Vol**.** 38, **No.** 15, **pp.** 1699-1712**.** https://doi.org/10.1016/S0020-7225(99)00134-2

Chamkha, A. J. (1997b): MHD-free convection from a vertical plate embedded in a thermally stratified porous medium with Hall effects, Applied Mathematical Modelling, Vol. 21, No. 10, pp. 603-609. https://doi.org/10.1016/S0307-904X(97)00084-X

Chamkha, A.J. and Khaled, A.A. (2000): Hydromagnetic combined heat and mass transfer by natural convection from a permeable surface embedded in a fluid-saturated porous medium, International Journal of Numerical Methods for Heat & Fluid Flow, Vol. 10, No. 5, pp. 455-477. https://doi.org/10.1108/09615530010338097.

Darcy, H. (1856), *Les fontaines publiques de la ville de Dijon*, Dalmont, Paris.

Das, K. (2012): Slip effects on heat and mass transfer in MHD micropolar fluid flow over an inclined plate with thermal radiation and chemical reaction, International Journal for Numerical Methods in Fluids, Vol. 70, pp. 96–113.

Doh, D. H. and Muthtamilselvan, M. (2017): Thermophoretic particle deposition on magnetohydrodynamic flow of micropolar fluid due to a rotating disk, International Journal of Mechanical Sciences, Vol. 130, pp. 350-359. https://doi.org/10.1016/j.ijmecsci.2017.06.029.

Dufour, L. (1873), *Ann. Phys*., 148, 490.

Eringen, A.C. (1966): Theory of micropolar fluids. Journal of Mathematics and Mechanics, Vol. 16, pp.1–18.

Eringen, A.C. (1972): Theory of thermomicrofluids, Journal of Mathematical Analysis and Applications, Vol. 38, pp. 480–496.

Ersoy, H. V. (1999): MHD flow of an Oldroyd-B fluid between eccentric rotating disks, International Journal of Engineering Science, Vol. 37 No. 15, pp. 1973–1984.

Ezzah, L.A., Syakila, A., Pop, I. (2014): Flow over a permeable stretching sheet in micropolar nanofluids with suction, AIP Conference Proceedings, Vol. 27, pp. 428–433.

Feroz, N., Islam, S., Shah, Z., Farooq, M., Nawaz, R., Ullah, H., Suleman, M. (2019): Micropolar Nanofluid Flow in Vertical Stretched Surface with Thermophoresis Effect and Brownian Motion, International Journal of Mathematics and Computer Science, Vol. 14 No. 4, pp. 975–992.

Gonzalez-Pinto, S., Montijano, J. I., Randez, L. (1995): Iterative schemes for three-stage implicit Runge-Kutta methods, Applied Numerical Mathematics, Vol. 17, pp. 363-382.

Hayat, T., Khan, M.I., Waqas, M., Alsaedi, A., Khan, M.I. (2017): Radiative flow of micro-polar nano-fluid accounting thermophoresis and Brownian moment, International Journal of Hydrogen Energy, Vol. 42 No. 26, pp. 16821–16833. https://doi.org/10.1016/j.ijhydene.2017.05.006

Hazarika, S., Ahmed, S., Chamkha, A. J. (2021): Investigation of Nanoparticles Cu, Ag and Fe_3O_4 on Thermophoresis and Viscous Dissipation of MHD Nanofluid over a Stretching Sheet in a Porous Regime: A Numerical Modelling, Mathematics and Computers in Simulation, Vol. 182, pp. 819-837. https://doi.org/10.1016/j.matcom.2020.12.005

Hazarika, S. and Ahmed, S. (2021): Study of Carbon Nanotubes with Casson Fluid in a Vertical Channel of Porous Media for Hydromagnetic Drag Force and Diffusion-Thermo, Journal of Scientific Research, Vol. 13 No. 1, pp. 31-45. https://doi.org/10.3329/jsr.v13i1.47458.

Hazarika, S., Ahmed, S., Yao, Shao-Wen (2021): Investigation of Cu–water nano-fluid of natural convection hydro-magnetic heattransport in a Darcian porous regime with diffusion-thermo, Applied Nanoscience. https://doi.org/10.1007/s13204-020-01655-w

Hollinger, S. t. and Lücke, M. (1995): Influence of the Dufour effect on convection in binary gas mixtures, Physical Review E, Vol. 52, pp. 642–657. https://doi.org/10.1103/PhysRevE.52.642.

Hsiao, K.L. (2017): Micropolar nanofluid flow with MHD and viscous dissipation effects towards a stretching sheet with multimedia feature, International Journal of Heat & Mass Transfer, Vol. 112, pp. 983-990. https://doi.org/10.1016/j.ijheatmasstransfer.2017.05.042.

Kasim, A.R.M., Mohammad, N.F., Shafie, S. (2013): Unsteady MHD mixed convection flow of a micropolar fluid along an inclined stretching plate, Heat Transfer- Asian Research, Vol. 42, pp. 89–99. https://doi.org/10.1002/htj.21034

Khan, N. A., Aziz, S., Khan, N.A. (2014): Numerical Simulation for the Unsteady MHD Flow and Heat Transfer of Couple Stress Fluid over a Rotating Disk, *PLoS ONE*, Vol. 9 No. 5, e95423. https://doi.org/10.1371/journal.pone.0095423.

Modather, M., Rashad, A. M., Chamkha, A. J. (2009): An analytical study of MHD heat and mass transfer oscillatory flow of a micropolar fluid over a vertical permeable plate in a porous medium, Turkish J. Eng. Env. Sci. Vol. 33, pp. 245 – 257.

Muhammad, R., Dong, C. J., Nadeem, U. (2017): Partial slip effect in the flow of MHD micropolar nanofluid flow due to a rotating disk - A numerical approach, Results in Physics. https://doi.org/:10.1016/j.rinp.2017.09.002.

Mustafa, M. (2017): MHD nanofluid flow over a rotating disk with partial slip effects: Buongiorno model, International Journal of Heat & Mass Transfer, Vol. 108, pp. 1910-1916. https://doi.org/10.1016/j.ijheatmasstransfer.2017.01.064.

Qukaszewicz, G. (1999): Micropolar Fluids: Theory and Application, Springer: Berlin/Heidelberg, Germany.

Rashad, A. M., and Chamkha, A. J. (2013): Unsteady heat and mass transfer by MHD mixed convection flow from a rotating vertical cone with chemical reaction and Soret and Dufour effects, The Canadian Journal of Chemical Engineering, Vol. 92, no. 4, pp. 758-767. https://doi.org/10.1002/cjce.21894.

Rashad, A. M., Abbasbandy, S., and Chamkha, Ali J. (2014): Mixed Convection Flow of a Micropolar Fluid over a Continuosly Moving Vertical Surface Immersed in Thermally and Solutally Stratified Medium with Chemical Reaction, Journal of the Taiwan Institute of Chemical Engineers, Vol. 45, pp. 2163-2169. https://doi.org/10.1016/j.jtice.2014.07.002.

Rauf, A., Ashraf, M., Batool, K., Hussain, M., Meraj, M. A. (2015): MHD flow of a micropolar fluid over a stretchable disk in a porous medium with heat and mass transfer, AIP Advances, Vol. 5, No. 7, pp. 1-15. https://doi.org/10.1063/1.4927501.

Reddy, P. S., and Chamkha, A. J. (2016): Soret and Dufour Effects on MHD Heat and Mass Transfer Flow of a Micropolar Fluid with Thermophoresis Particle Deposition, Journal of Naval Architecture and Marine Engineering, Vol. 13, no. 1, pp. 39-50. https://doi.org/10.3329/jname.v13i1.23974 .

Reddy, P. S., Sreedevi, P., and Chamkha, Ali. J. (2017): MHD boundary layer flow, heat and mass transfer analysis over a rotating disk through porous medium saturated by Cu-water and Ag-water nanofluid with chemical reaction, Powder Technology, Vol. 307, pp. 46-55. https://doi.org/10.1016/j.powtec.2016.11.017.

Rehman, F., Khan, M. I., Sadiq, M., Malook, A. (2017): MHD flow of carbon in micropolar nanofluid with convective heat transfer in the rotating frame, Journal of Molecular Liquids, Vol. 231, pp. 353-363. https://doi.org/10.1016/j.molliq.2017.02.022.

Sabir, Z., Ayub, A., Guirao, Juan L. G., Bhatti, S., Shah, S. Z. H. (2020): The Effects of Activation Energy and Thermophoretic Diffusion of Nanoparticles on Steady Micropolar Fluid along with Brownian Motion, Advances in Materials Science and Engineering, Vol. 2020, Article ID 2010568. https://doi.org/10.1155/2020/2010568.

Sheikholeslami, M., Rashidi, M. M., Firouzi, F., Houman, B. R., Domairry, G. (2015): The steady nanofluid flow between parallel plates considering thermophoresis and Brownian effects, Journal of King Saud University Science, Vol. 4, pp. 380-389. https://doi.org/10.1016/j.jksus.2015.06.003.

Takhar, H. S., Chamkha, A. J., Nath, G.(1999): Unsteady flow and heat transfer on a semi-infinite flat plate with an aligned magnetic field, International Journal of Engineering Science, Vol. 37, No. 13, pp. 1723-1736. https://doi.org/10.1016/S0020-7225(98)00144-X

Takhar, H. S., Chamkha, A. J., Nath, G. (2000): Combined heat and mass transfer along a vertical moving cylinder with a free stream, Heat and Mass transfer, Vol. 36, pp. 237-246. https://doi.org/10.1007/s002310050391

Takhar, H.S., Chamkha, A.J., Nath, G. (2003): Unsteady mixed convection flow from a rotating vertical cone with a magnetic field. *Heat and Mass Transfer* **39,** 297–304. https://doi.org/10.1007/s00231-002-0400-1

Zemedu, C. and Ibrahim, W. (2020): Nonlinear Convection Flow of Micropolar Nanofluid due to a Rotating Disk with Multiple Slip Flow, Mathematical Problems in Engineering, Vol 2020, Article ID 4735650. https://doi.org/10.1155/2020/4735650.

Zueco, J., Ahmed, S. and Gonzalez, L. M. L. (2017): 2-D unsteady free convective heat and mass transfer Newtonian Hartmann flow with thermal diffusion and Soret effects: Network model and finite differences, International Journal of Heat and Mass Transfer, Vol. 110, pp. 467-475. https://doi.org/10.1016/j.ijheatmasstransfer.2017.03.046